A BUILDING-INTEGRATED PHOTOVOLTAIC PROTOTYPE FOR CALCULATING SOLAR ORIENTATION AND SOLAR INSOLATION

Manish Dixit[1], Wei Yan[1]
[1]Texas A&M University, College Station, USA

ABSTRACT

The renewable energy systems such as a Building Integrated Photovoltaic (BiPV) installed as building components often influence the aesthetic quality of a building. This becomes crucial especially in the case of a sun-tracking photovoltaic system that is installed on a wall or a roof of the building. Hence, it is important for a building designer to calculate and visualize the movement of a sun-tracking BiPV over an entire day. Moreover, there is a lack of a reasonably accurate but quick method to estimate the amount of global solar insolation received at a given location. Existing global insolation models require data that are either unavailable or difficult to obtain. Such models are not very helpful to building professionals interested in determining the economic feasibility of a BiPV system based on the amount of renewable energy it generates.

A Building Information Model can perform both the visualization of BIPV's movement and the global solar insolation calculation to help building professionals compare the feasibility of various BiPV options. This paper develops a BiPV prototype to visualize the movement of sun-tracking BiPV modules and to calculate the global insolation using readily available weather information. The BiPV prototype utilizes the Autodesk Revit Architecture as a BIM platform. We used a solar insolation model proposed in the literature to develop the prototype and computed global solar insolation for twelve locations in the United States. The calculated values of global solar insolation are compared with the measured insolation data to validate the results. The measured global insolation values are sourced from the Atmospheric Science Data Center (ASDC), National Aeronautics and Space Administration). Finally, we discussed the significance of the research and identified the future research needs.

INTRODUCTION

Building operations alone consumed over 41% of the United States' energy in 2010 resulting in approximately 40% of the nation's annual carbon emission (BEDB, 2012). Approximately half of this carbon emission originated from the residential building sector (BEDB, 2012). According to Torcellini et al. (2006), an effective technique to offset increasing energy consumption is to equip buildings with renewable energy systems enough to create a net-zero energy balance. Major net-zero energy building design strategies include applying active and passive energy saving techniques to optimize the energy usage and installing renewable energy options to offset the remaining energy demand (Hernandez and Kenny, 2010; Dixit et al., 2014; Snow and Prasad, 2011). A balance of optimized energy usage and renewable energy generation is critical to creating a net-zero energy built environment (Marszal et al., 2011). Due to extensive research focused on building energy use optimization, the operating energy of buildings is being gradually reduced (Dixit et al., 2010; Dixit et al., 2012). However, the application of renewable energy systems such as photovoltaics (PVs) to buildings remains limited (Snow and Prasad, 2011).

Most photovoltaic systems applied to a building are rack-mounted rather than building integrated (Torcellini et al., 2006; Snow and Prasad, 2011). According to James et al. (2011), by the end of 2009, BiPV systems worldwide represented only 1% of the total installed PV system capacity. A rack-mounted PV system is attached to a building, whereas a building-integrated photovoltaic (BiPV) system is integrated into building elements such as walls, roofs, canopies etc. A BiPV system is preferred over a rack mounted PV system because of added advantages such as protection from heat, cold, and rain (Kaan and Reijenga, 2004; Snow and Prasad, 2011). Installing a BiPV system may also provide cost benefits since it serves as both a building element and an energy generator (Tsoutsos et al., 2005; Omer et al., 2003; Snow and Prasad, 2011). Because BiPV systems replace building components, their design, positioning, and layout can alter the aesthetic quality of a building (Snow and Prasad, 2011). Studies (Xuan et al., 2007; Dixit and Yan, 2012) suggested analyzing both the aesthetical and technical performances while making a selection of BiPV systems. A visually appealing BiPV system can also help enhance the value of a building (Kaan and Reijenga, 2004). Three aspects of a BiPV system are important to its industry-wide acceptance: (1) aesthetical quality; (2) energy production capacity; and (3) installation cost (Reijenga, 1996; Kaan and Reijenga, 2004; Xuan et al., 2007; Dixit and Yan, 2012). Changing BiPV module size, orientation, layout, and position to maximize energy generation can affect a building's architectural quality (Xuan et al., 2007; Dixit and Yan, 2012). This is particularly important in the case of a sun-tracking BiPV module whose orientation would differ throughout the day (Dixit and Yan, 2012). Therefore, a balance of aesthetics and the energy generation potential must be sought while designing a building with a BiPV system (Kaan and Reijenga, 2004; Xuan et al., 2007; Snow and Prasad, 2011; Dixit and Yan, 2012). Another important issue is the limited expertise of building designers, constructors, and developers in effectively applying BiPV systems to buildings (Kaan and Reijenga, 2004). A tool that is well integrated into a widely-used design and construction technology can help building design and construction professionals to analyze, select, and integrate a BiPV system into the building fabric (Dixit and Yan, 2012).

This paper focuses on developing a generic Building Information Modeling (BIM)-based BiPV prototype to visualize the movement of sun-tracking BiPV roof tiles. The prototype also calculates the daily energy generation by the selected BiPV system for a given location. The application of BIM to building design and construction is increasing and this technology is seen as an excellent tool to design, construct, and maintain a building as a single system.

LITERATURE REVIEW

Building-integrated Photovoltaic (BiPV) Systems

Among popular renewable energy systems installed in a building are PV systems that generate electricity using solar energy. Primarily, there are three types of PV systems: (1) monocrystalline; (2) polycrystalline; and (3) non-crystalline or amorphous (Xuan et al., 2007; Snow and Prasad, 2011; Dixit and Yan, 2012). The monocrystalline modules are dark in color with a better energy conversion efficiency (14-17%) but a higher installation cost, whereas the blue-colored polycrystalline modules cost less but provide a lower energy conversion efficiency (12-14%). The amorphous modules are transparent and have a poor efficiency of energy conversion (Xuan et al., 2007; Snow and Prasad, 2011). Most of these systems are building-applied photovoltaics (BAPV) installed on racks on building rooftops or on building surroundings and are not well-integrated into the building as building components (Snow and Prasad, 2011). BiPV systems are designed and installed as building components and are completely integrated into the building (Kaan and Reijenga, 2004; Xuan et al., 2007; Snow and Prasad, 2011; Dixit and Yan, 2012). According to studies (Xuan et al., 2007; Snow and Prasad, 2011; Dixit and Yan, 2012), BiPV systems have financial and functional advantages over BAPV systems. A BiPV system serves dual purposes and, unlike BAPV systems, avoids investing in two different components. For instance, a roof installed with BiPV shingles saves the cost of installing regular shingles, which would have been necessary in the case of a BAPV system. BiPV building components also provide additional protection from heat, cold, and rain. According to Snow and Prasad (2011), BiPV systems can also help control noise and enhance a building's thermal performance. Because they are integrated into a building, they can be used to enhance the aesthetic quality of the building (Xuan et al., 2007). BiPV systems' color, texture, and module shapes can complement the architectural character of buildings. Building components such as wall cladding, glazing panels, roof tiles, canopies, etc. can be designed as photovoltaic modules (Kaan and Reijenga, 2004; Xuan et al., 2007; Snow and Prasad, 2011). Unlike BiPV, a BAPV system may not be visually appealing to the designer due to its add-on appearance (Snow and Prasad, 2011).

Net-zero Energy Buildings and BiPV

A net-zero energy building is designed to optimize its energy performance and to offset remaining energy usage with onsite or offsite renewable energy (Marszal et al., 2011). The total energy usage of a building over its service life is made of embodied and operating energy. The total energy consumed in constructing the building is called its embodied energy (Dixit et al., 2013; Dixit et al., 2015). The operating energy is used in air-conditioning, heating, lighting, providing hot water, and powering building equipment (Dixit et al., 2012). A design for a net-zero energy building must focus on optimizing operating as well as embodied energy (Marszal et al., 2011). The optimized energy demand of the building can be met using renewable energy sources. A BiPV system provides an excellent opportunity to embed renewable energy generation capability into a building design. Because design decisions can control most of the energy and cost expenditure of a building, Snow and Prasad (2011) recommended considering BiPV integration during the early design phase.

Architectural Issues of BiPV

Because BiPV systems are integral to buildings, they can affect the architectural quality of the buildings (Dixit et al., 2012; Sick and Erge, 2014). According to Kaan and Reijenga (2004), most PV systems remain added features to buildings due to their inadequate integration into the building design. Even though most PV systems demonstrate excellent potential of enhancing architectural qualities, they are hardly used by designers for "architectural expression" (Kaan and Reijenga, 2004). One of the major concerns for most designers is to integrate BiPV systems into design without adversely affecting the building aesthetics (Sick and Erge, 2014; Kaan and Reijenga, 2004). Sick and Erge (2014) suggested a strong engineer-architect collaboration to effectively integrate BiPV systems into a building design. According to Snow and Prasad (2011) and Xuan et al. (2007), BiPV systems would demonstrate excellent financial feasibility and social acceptance if a thoughtful design can enhance both the efficiency (technical aspects) and the aesthetics. A major dilemma faced by architects while designing with BiPV systems is to decide whether to enhance aesthetical character or improve energy generation of modules. For instance, orienting BiPV modules in a particular direction may provide increased energy generation but may influence the building aesthetics adversely (Xuan et al., 2007). Among important architectural concerns are the design, layout, and positioning of BiPV arrays (Snow and Prasad, 2011; Xuan et al., 2007). BiPV manufacturing industry and market are responding to architectural needs by providing a variety of BiPV products ranging from individual bendable modules in different colors to the entire solar roof assembly (Photovoltaics Bulletin, 2003). Related software tools for simulating the behavior and energy performance of BiPV systems can help designers and engineers to innovatively integrate them into a building (Dixit and Yan, 2012).

Energy Generation Issues of BiPV

Three issues that can influence the total energy generation by a BiPV system are worth discussing. The first issue pertains to the selection of a BiPV system. A variety of BiPV systems have been proposed ranging from traditional mono and polycrystalline to thin film photovoltaics each having a different energy conversion efficiency (Xuan et al., 2007; Snow and Prasad, 2011). Chow (2010) discussed air-type and liquid-type hybrid systems that combined a photovoltaic system and a thermal solar system to generate not only electricity but also heat. Each of these systems generates a different amount of electricity based on the material and technology used. The second issue is the design and layout of BiPV systems that affect the amount of sunlight reaching the solar modules (Kumar and Umananda, 2005; Xuan et al., 2007; Norton et al., 2011). A roof-based photovoltaic array may receive more sunlight than a wall-integrated one (Dixit and Yan, 2012). Similarly, in some geographic locations, a flat roof with horizontal solar panels may collect more sunlight than a pitched roof (Norton et al., 2011). The static and sun-tracking nature of solar modules also affects the amount of energy generation. The amount of solar radiation received by a surface is maximum when sunrays are perpendicular to the surface (Chemisana, 2011; Duffie and Beckman, 2013). The solar radiation on a static or fixed solar module varies throughout the day due to the movement of the sun. A sun-tracking solar module orients itself towards the sun throughout the day and maximizes the amount of solar radiation received by the module. A sun-tracking module tracks the sun on single or dual axes. The solar altitude and azimuth angles determine the position of the sun in the sky. A single axis-tracking module may track sun along the altitude or azimuth angle. A dual axis module, however, tracks the sun along both the angles. There is a strong need to develop tools to visualize the behavior of PV panels tracking the sun on single or dual axes (Dixit and Yan, 2012).

The amount of solar radiation received just outside the earth's atmosphere remains constant (Kumar and Umananda, 2005; Duffie and Beckman, 2013). However, solar radiation received by a geographic location on earth is governed by the atmospheric conditions such as weather and pollution (Kumar and Umananda, 2005; Dixit and Yan, 2012). The time dependent variation in the solar radiation due to the sun's movement can be predicted using geometric calculations. The weather dependent variation, however, is difficult to determine and can only be calculated using historical weather data (Kumar and Umananda, 2005). A factor known as the *sky clearness index* is used to account for any atmospheric condition that may influence the amount of solar radiation reaching a location on the globe. According to Kumar and Umananda (2005), various models to calculate the *sky clearness index* have been proposed, which are either expensive, time-consuming, or require weather data that is not readily available. This poses another challenge to successful application of BiPV technology to a building (Dixit and Yan, 2012).

RESEARCH GOAL AND SIMULATION

From the review of literature, two requirements relating to BiPV research clearly stand out. First, widely used design and construction technologies such as BIM are currently lacking a capability to visualize the movement of a sun-tracking BiPV system. Such a capability is essential to design decisions regarding BiPV installation in a building. Second, a tool for computing the amount of solar electricity generation at a given location needs to be integrated into a widely used design and construction technology (e.g. BIM). Such integration would help architects, constructors, and property developers to use the information model to compute energy generation and calculate payback time to determine the economic feasibility of BiPV systems. A BIM authoring tool added with both the visualization and solar energy calculation capabilities can provide an excellent platform to compare and select a BiPV system.

We used the Autodesk Revit Architecture as the BIM authoring tool. To enable visualization of BiPV modules, a parametric family of dual axis sun-tracking roof tiles was developed and nested into a roof family. The BiPV family is a nested family involving roof attachments and solar modules with parameters representing solar altitude and azimuth angles. The BiPV family was developed in a way to facilitate the free movement of each individual panel and avoid solar modules to cast shadows on each other. The Revit BiPV family was then loaded into a residential Building Information Model.

For calculating solar altitude and azimuth angles, we referred to the equations provided by Duffie and Beckman (2013). A probabilistic model based on the periodicity of sky clearness index was developed for

North America using the method proposed by Kumar and Umananda (2005). In this method, a *sky clearness index* model is developed using measured solar insolation and precipitable water vapour data for known locations. The model utilizes Fourier series to calculate Fourier constants, which are used to compute the *sky clearness index* for a desired location. Twelve geographic locations in North America within the latitude range of 8.97°-31.53°N and the longitude range of 79.53°-155.07°W were used to develop the calculation model. Table 1 lists the twelve locations used in the model development. Using the model, we calculated the monthly average values of the *sky clearness index* and the amount of solar insolation for twelve other locations in the United States. These twelve locations were different from the ones used in developing the calculation model. To validate the calculation model, we compared the results to the last 20 years average values of clearness index and solar insolation measured by the Atmospheric Science Data Center (ASDC), National Aeronautics and Space Administration).

Table 1
Twelve locations used in developing the sky clearness index model

Location	Latitude	Longitude
Panama City	8.97	-79.53
Guatemala City	14.62	-90.5
Mexico City	19.43	-99.12
Hilo, HI	19.72	-155.07
Durango, MX	24.017	-104.66
Brownsville, TX	25.9	-97.43
Naples, FL	26.13	-81.8
Laredo, TX	27.53	-99.47
Orlando	28.4	-81.3
San Antonio	29.42	-98.5
New Orleans	29.95	-90.25
Albany, GA	31.53	-84.18

Both the visualization and solar insolation algorithms were integrated as an add-in tool into the Revit Architecture model using Revit's application programming interface (API). We called this tool a BiPV prototype. The BiPV prototype receives user inputs through a graphical user interface (GUI) developed in the C# programming language. For visualizing the movement of BiPV modules throughout the day, both the geographic location and time data were sought through the GUI. The solar insolation calculation algorithm provides average monthly values using the latitude and longitude data entered by the user. The calculation of solar insolation was programed in the prototype. To access the clearness indices, the BiPV prototype interacts with a calculation spreadsheet and gets the clearness index values using the geographic location and date information. The spreadsheet was developed based on the sky clearness index calculation model as proposed by Kumar and Umananda (2005). Using the calculated values of sky clearness indices, the amount of solar insolation reaching a particular location was determined.

RESULTS AND DISCUSSION

Results

The parametric nested family is loaded into a Revit project of a house to model the movement of sun-tracking solar modules installed on the roof. Figures 1 and 2 illustrate the Revit project and the nested parametric BiPV family. The length, width, and the pitch of the roof are mapped to the parameters of the parametric BiPV family. Figure 3 shows the GUI window that seeks the required user inputs. The BiPV prototype gets solar altitude and azimuth angle parameters from the BiPV family, computes their new values based on the entered location, date, and time, and sets the new values. Upon completion of the process, the prototype modifies the orientation of solar modules and shows the new orientation in the Revit model. The pitch and the size of the roof can be modified as required. Using the calculated solar positions of the sun-tracking solar panels, their movement can be simulated for an entire day.

Figure 1 Building model with BiPV roof family

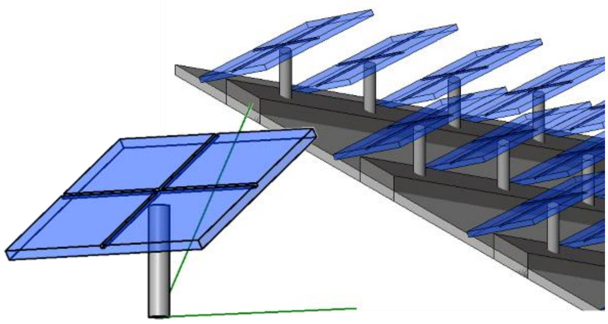

Figure 2 Nested parametric Revit BiPV family

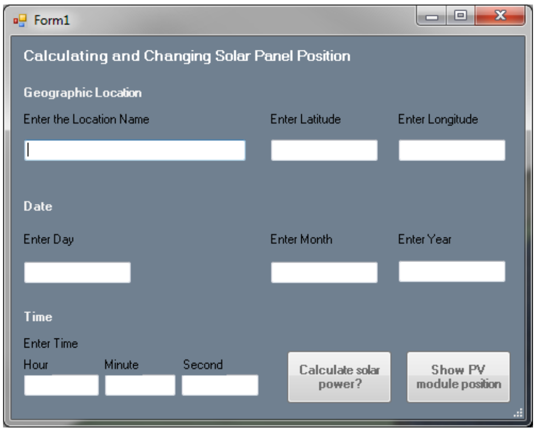

Figure 3 GUI window for user inputs

Table 2 and 3 list the calculated values of average monthly clearness indices and solar insolation, respectively for the 12 study locations. The calculated values of clearness index were within 5% and -7% of the measured values. The cases of Miami (Florida) (-7%), El Paso (Texas) (-6%), and Hattiesburg (Mississippi) (5%) showed larger differences. Remaining locations demonstrated results within 5% of the measured values. Such error is reasonable in making predictions about the solar insolation received by a BiPV system. When compared with the measured values of the solar insolation provided by the ASDC website, the calculated values were within 7% and -5% of the measured values. Locations such as Baton Rouge (Louisiana) demonstrated very little difference between the calculated and measured values of solar insolation. Figure 4 presents four plots of calculated and measured monthly values of solar insolation for Miami, Hattiesburg, Baton Rouge, and El Paso. As seen in Figure 4, the calculated values closely followed the measured values obtained from the ASDC website.

Discussion

This paper, in part, focused on investigating the modelling of the movement of sun-tracking BiPV panels on dual axes. Such modelling is crucial for analyzing the impact of a BiPV system over building aesthetics. Although we developed a prototype for a dual axis sun tracking, the same process can be used to create a single axis sun-tracking BiPV system. Similarly, we created a roof-based Revit family to test the prototype, but interested researchers or professionals can apply the same process to visualize the movement of other canopy or wall-based BiPV systems.

The calculation of solar insolation on dual axis sun-tracking BiPV modules produced results having reasonable accuracy compared with measured data. Both the calculated and measured solar insolation and clearness indices demonstrated a strong positive correlation. Figures 4 and 5 illustrate the scatter plots between the calculated and measured values for Miami and Baton Rouge.

The calculated values for Miami showed larger differences with the measured values probably due to the proximity to the sea. In addition, the calculation model utilized the locations not only in the United States but also in Mexico, Guatemala, and Panama causing larger differences. Although this model calculated monthly average values of solar insolation, it can also be applied to compute daily average insolation. Such a model is very useful to building designers, constructors, and property developers to make a decision based on the monthly energy generation and payback time of a BiPV system.

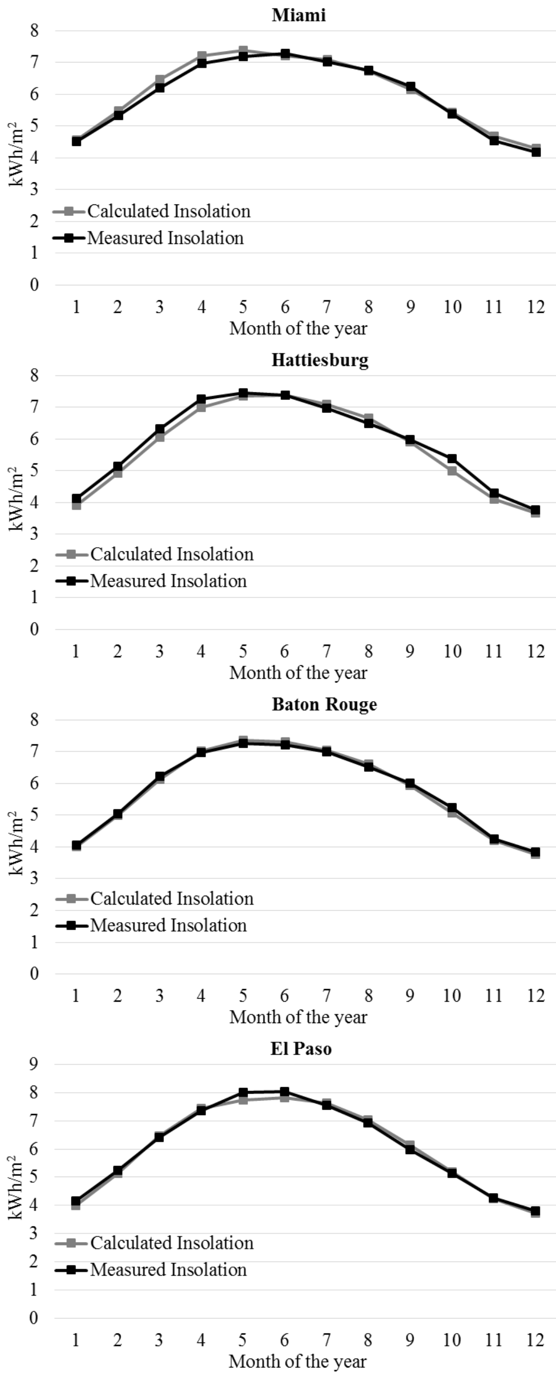

Figure 3 Comparison of the calculated and measured values of solar insolation

Table 2
Comparison of calculated and measured clearness indices in the study locations

Location		Calculated (K_{cal}) and measured (K_{md}) clearness indices (Average monthly)											
		Jan	Feb	Mar	Apr	May	Jun	Jul	Aug	Sep	Oct	Nov	Dec
Jacksonville, FL	K_{cal}	0.69	0.70	0.70	0.69	0.66	0.64	0.63	0.63	0.64	0.67	0.69	0.69
	K_{md}	0.70	0.71	0.70	0.70	0.66	0.63	0.62	0.63	0.65	0.66	0.68	0.69
Austin, TX	K_{cal}	0.70	0.71	0.71	0.69	0.66	0.65	0.64	0.64	0.65	0.67	0.70	0.70
	K_{md}	0.72	0.73	0.74	0.70	0.67	0.66	0.65	0.65	0.65	0.69	0.71	0.71
Miami, FL	K_{cal}	0.69	0.70	0.70	0.69	0.67	0.64	0.64	0.63	0.65	0.67	0.69	0.69
	K_{md}	0.67	0.67	0.66	0.66	0.64	0.64	0.63	0.63	0.64	0.64	0.65	0.66
El Paso, TX	K_{cal}	0.72	0.74	0.75	0.73	0.69	0.68	0.68	0.67	0.68	0.70	0.73	0.72
	K_{md}	0.72	0.74	0.73	0.72	0.71	0.70	0.67	0.65	0.64	0.67	0.70	0.72
Mobile, AL	K_{cal}	0.69	0.70	0.70	0.69	0.66	0.64	0.63	0.63	0.65	0.67	0.69	0.70
	K_{md}	0.70	0.70	0.69	0.69	0.66	0.65	0.63	0.62	0.65	0.69	0.70	0.69
Houston, TX	K_{cal}	0.69	0.70	0.70	0.68	0.66	0.64	0.63	0.63	0.65	0.67	0.69	0.70
	K_{md}	0.71	0.71	0.71	0.67	0.64	0.62	0.61	0.61	0.64	0.66	0.70	0.70
Baton Rouge, LA	K_{cal}	0.69	0.70	0.70	0.68	0.66	0.64	0.63	0.63	0.65	0.67	0.69	0.70
	K_{md}	0.69	0.70	0.70	0.68	0.65	0.63	0.62	0.62	0.64	0.68	0.68	0.70
Huntsville, TX	K_{cal}	0.69	0.70	0.70	0.68	0.66	0.64	0.64	0.63	0.65	0.67	0.69	0.70
	K_{md}	0.71	0.72	0.72	0.68	0.66	0.63	0.62	0.62	0.66	0.68	0.70	0.71
Dothan, AL	K_{cal}	0.69	0.70	0.70	0.69	0.66	0.64	0.63	0.63	0.65	0.67	0.70	0.70
	K_{md}	0.71	0.72	0.72	0.69	0.67	0.65	0.62	0.63	0.66	0.70	0.71	0.71
Thomasville, GA	K_{cal}	0.69	0.70	0.70	0.69	0.66	0.64	0.63	0.63	0.64	0.67	0.69	0.70
	K_{md}	0.71	0.71	0.71	0.69	0.66	0.63	0.62	0.62	0.64	0.68	0.69	0.70
Hattiesburg, MS	K_{cal}	0.69	0.70	0.70	0.69	0.66	0.64	0.63	0.63	0.65	0.67	0.69	0.70
	K_{md}	0.72	0.72	0.72	0.71	0.66	0.64	0.62	0.61	0.64	0.71	0.71	0.71
Alexandria, LA	K_{cal}	0.69	0.70	0.70	0.68	0.66	0.64	0.63	0.63	0.65	0.67	0.69	0.70
	K_{md}	0.71	0.72	0.71	0.68	0.66	0.63	0.61	0.61	0.64	0.69	0.71	0.71

Table 3
Comparison of calculated and measured solar insolation in the study locations

Location		Calculated (I_{cal}) and measured (I_{md})solar insolation in kWh/m^2 (Average monthly)											
		Jan	Feb	Mar	Apr	May	Jun	Jul	Aug	Sep	Oct	Nov	Dec
Jacksonville, FL	I_{cal}	4.02	4.98	6.11	7.03	7.36	7.30	7.04	6.59	5.90	5.03	4.18	3.76
	I_{md}	4.13	5.11	6.26	7.20	7.39	7.28	7.03	6.64	6.04	5.15	4.26	3.77
Austin, TX	I_{cal}	4.08	5.07	6.19	7.05	7.37	7.39	7.26	6.75	5.99	5.09	4.25	3.81
	I_{md}	4.26	5.27	6.59	7.28	7.55	7.64	7.32	6.85	6.12	5.33	4.43	3.92
Miami, FL	I_{cal}	4.55	5.47	6.47	7.20	7.38	7.21	7.09	6.73	6.16	5.43	4.67	4.29
	I_{md}	4.51	5.34	6.19	6.98	7.19	7.29	7.02	6.76	6.24	5.37	4.54	4.18
El Paso, TX	I_{cal}	4.00	5.14	6.47	7.42	7.74	7.82	7.62	7.04	6.13	5.18	4.25	3.73
	I_{md}	4.15	5.23	6.41	7.36	8.01	8.02	7.55	6.91	5.97	5.14	4.28	3.82
Mobile, AL	I_{cal}	3.98	4.96	6.10	7.02	7.36	7.34	7.06	6.62	5.92	5.04	4.17	3.73
	I_{md}	4.13	5.05	6.18	7.16	7.44	7.46	7.19	6.59	6.11	5.35	4.34	3.82
Houston, TX	I_{cal}	4.09	5.06	6.17	7.03	7.35	7.32	7.14	6.67	5.97	5.10	4.26	3.83
	I_{md}	4.30	5.22	6.39	6.98	7.21	7.09	6.94	6.49	6.08	5.17	4.46	3.97
Baton Rouge, LA	I_{cal}	4.01	4.99	6.12	7.01	7.35	7.32	7.06	6.62	5.94	5.06	4.20	3.76
	I_{md}	4.05	5.04	6.23	6.98	7.27	7.22	6.99	6.52	6.02	5.25	4.25	3.84
Huntsville, TX	I_{cal}	3.99	4.97	6.10	7.00	7.34	7.35	7.16	6.67	5.93	5.03	4.17	3.73
	I_{md}	4.21	5.21	6.38	7.05	7.37	7.29	7.01	6.56	6.15	5.25	4.38	3.89
Dothan, AL	I_{cal}	3.93	4.93	6.08	7.03	7.37	7.38	7.11	6.65	5.91	5.01	4.12	3.68
	I_{md}	4.08	5.09	6.32	7.07	7.52	7.55	7.08	6.64	6.13	5.34	4.29	3.78
Thomasville, GA	I_{cal}	3.96	4.95	6.08	7.02	7.36	7.32	7.05	6.59	5.89	5.01	4.15	3.71
	I_{md}	4.17	5.15	6.32	7.11	7.38	7.22	7.00	6.52	6.03	5.27	4.30	3.83
Hattiesburg, MS	I_{cal}	3.92	4.91	6.06	6.99	7.35	7.37	7.09	6.65	5.91	5.00	4.11	3.66
	I_{md}	4.13	5.13	6.32	7.26	7.45	7.37	6.98	6.49	5.97	5.38	4.30	3.77
Alexandria, LA	I_{cal}	3.92	4.91	6.05	6.98	7.34	7.35	7.09	6.64	5.90	4.99	4.11	3.66
	I_{md}	4.09	5.11	6.28	7.04	7.46	7.31	6.96	6.50	5.94	5.27	4.29	3.78

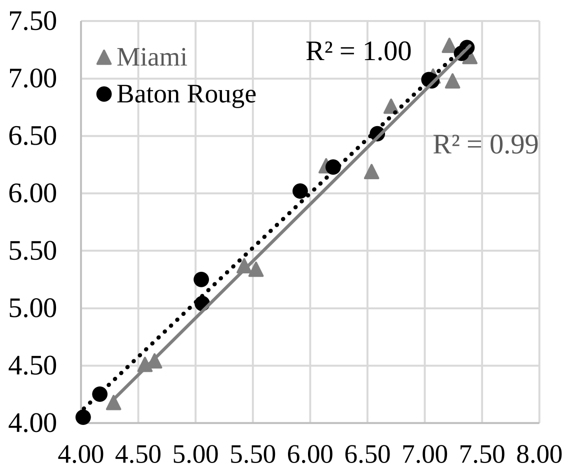

Figure 4 Correlation between the calculated and measured values of solar insolation (kWh/m²)

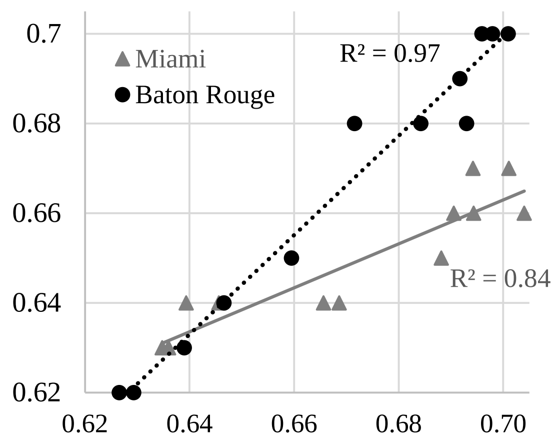

Figure 5 Correlation between the calculated and measured values of clearness index

CONCLUSIONS

In this paper, we proposed a BIM-integrated tool to visualize the movement of sun-tracking BiPV modules and calculate the amount of solar insolation for computing the solar electricity generated at a given location. This tool is significant to developing a comprehensive BIM-based net-energy analysis tool that can help building design and construction professionals to make informed decisions. Decisions regarding the selection of BiPV system based on building aesthetics and energy generation capability (economic feasibility) are easier to make with such a tool. Since this tool utilizes readily available weather data, it can be used for any location on the globe with a slight modification to the solar insolation model. In the future, we plan to include this tool into a life cycle-based net energy accounting system that can be integrated into BIM.

REFERENCES

BEDB (2012). Building Energy Databook, United States Department of Energy.

Chemisana, D. (2011). Building integrated concentrating photovoltaics: a review. Renewable and Sustainable Energy Reviews, 15(1), 603-611.

Chow, T. T. (2010). A review on photovoltaic/thermal hybrid solar technology. Applied Energy, 87(2), 365-379.

Dixit, M. K., & Yan, W. (2012). BIPV prototype for the solar insolation calculation, Gerontechnology, 11(2), 162.

Dixit, M. K., Culp, C. H., & Fernandez-Solis, J. (2015). Embodied Energy of Construction Materials: Integrating Human and Capital Energy into an IO-Based Hybrid Model. Environmental science & technology, 49(3), 1936-1945.

Dixit, M.K., Culp, C. H., & Fernández-Solís, J. L. (2013). System boundary for embodied energy in buildings: A conceptual model for definition. Renewable and Sustainable Energy Reviews, 21, 153-164.

Dixit, M.K., Culp, C.H., Lavy, S., & Fernández-Solís, J.L. (2014). Recurrent embodied energy and its relationship with service life and life cycle energy: a review paper. Facilities, 32(3/4), 160-181.

Dixit, M.K., Fernández-Solís, J. L., Lavy, S., & Culp, C. H. (2012). Need for an embodied energy measurement protocol for buildings: A review paper. Renewable and Sustainable Energy Reviews, 16(6), 3730-3743.

Dixit, M.K., Fernández-Solís, J., Lavy, S., & Culp, C.H. (2010). Identification of parameters for embodied energy measurement: A literature review. Energy and Buildings, 42 (8), 1238-1247.

Duffie, J. A., & Beckman, W. A. (1980). Solar engineering of thermal processes (Vol. 3). New York etc.: Wiley.

Hernandez, P., & Kenny, P. (2010). From net energy to zero energy buildings: Defining life cycle zero energy buildings (LC-ZEB). Energy and Buildings, 42(6), 815-821.

James, T., Goodrich, A., Woodhouse, M., Margolis, R., & Ong, S. (2011). Building-Integrated Photovoltaics (BIPV) in the residential sector: an analysis of installed rooftop system prices, Technical Report, NREL/TP-6A20-53103, National Renewable Energy Laboratory, Golden, CO, USA.

Kaan, H., & Reijenga, T. (2004). Photovoltaics in an architectural context. Progress in Photovoltaics: Research and Applications, 12(6), 395-408.

Kumar, R., & Umananda, L. (2005). Estimation of global radiation using clearness index model for sizing photovoltaic system, Renewable Energy, Vol. 30(15), pp. 2221-2233.

Marszal, A. J., Heiselberg, P., Bourrelle, J. S., Musall, E., Voss, K., Sartori, I., & Napolitano, A. (2011). Zero Energy Building–A review of definitions and calculation methodologies. Energy and Buildings, 43(4), 971-979.

NASA Surface Meteorology and Solar Energy website, http://eosweb.larc.nasa.gov

Norton, B., Eames, P. C., Mallick, T. K., Huang, M. J., McCormack, S. J., Mondol, J. D., & Yohanis, Y. G. (2011). Enhancing the performance of building integrated photovoltaics. Solar Energy, 85(8), 1629-1664.

Omer, S.A., Wilson, R., & Riffat, S.B. (2003). Monitoring results of two examples of building integrated PV (BIPV) systems in the UK, Renewable Energy, Vol. 28(9), 1387-1399, 2003.

Photovoltaics Bulletin, (2003). BIPV: Solar-friendly versus architectural aesthetic, Feature, Photovoltaics Bulletin, 2003(9), 7-9.

Reijenga, T.H. (1996). Photovoltaics in Architecture in The Netherlands: an Architect’s View, Progress in Photovoltaics: Research and Applications, Vol. 4(4), 279-294.

Sick, F. & Erge, T. (2014). Photovoltaics in buildings: a design handbook for architects and engineers. Fraunhofer Institute for Solar Energy Systems (FhG-ISE) Freiburg, Germany.

Snow, M., & Prasad, D. (2011). Building-integrated Photovoltaics (BIPV), EDG 68 MS, July 2011, environmentdesignguide.com.eu

Torcellini, P., Pless, S., Deru, M., & Crawley, D. (2006). Zero energy buildings: a critical look at the definition. National Renewable Energy Laboratory, Golden, CO, USA.

Tsoutsos, T., Frantzeskaki, N., Gekas, V. (2005). Environmental impacts from the solar energy technologies, Energy Policy, Vol. 33(3), pp. 289-296.

Xuan, X., & Zheng, X. (2007). Facade Design in Building Integrated Photovoltaics, In: Proceedings of ISES World Congress 2007, pp. 284-387.